Experimental characterization of tensile strength of steel and fibre rovings also under environmental conditioning

Giuseppe Maddaloni [a,b], Eliana Parcesepe [a,*], Annalisa Franco [b], Antonio Bonati [b], Antonio Occhiuzzi [b,c], Maria Rosaria Pecce [a,b]

[a] University of Sannio, Department of Engineering, Piazza Roma, 21, Benevento, 82100, Italy
[b] Construction Technologies Institute of the Italian National Research Council (ITC-CNR), Via Lombardia, 49, San Giuliano Milanese, 20098, MI, Italy
[c] University of Naples "Parthenope", Department of Engineering, Centro Direzionale, Isola C4, Naples, 80143, Italy

A B S T R A C T

The efficiency of the strengthening techniques by externally applied materials can be improved enhancing the debonding strength of the reinforcement from the support by the use of connectors (anchor spikes) consisting of unidirectional bundles of fibres embedded in concrete or masonry by means of organic or inorganic matrices. The use of connectors is suggested in various codes and guidelines of strengthening techniques by composite materials and provisions for their application are given, but currently there are no details for the qualification of the material. In order to investigate anchor spikes made of glass, basalt, aramid, carbon, PBO and steel, a large experimental campaign was carried out at the Materials and Structures Laboratory of the University of Sannio. The tests allowed to evaluate the mechanical characteristics (tensile strength, modulus of elasticity, deformation at the maximum load) of the anchor spikes constituted by only dry fibres, not impregnated, also as a result of environmental conditioning such as freezing and thawing, controlled humidity, alkaline and saline environment.

1. Introduction

Among many structural retrofitting techniques, in the last two decades the use of composite materials, with various types of fibres as carbon or glass ones but also stainless or galvanized steel ones, as strengthening material for masonry and reinforced concrete (RC) structures is becoming the most popular, thanks to their favourable properties as low weight, easy handling and application, high strength, immunity to corrosion, minimal disruption of occupancy.

In the continuous advancement and renewal of technical solutions, to solve some problems associated with epoxy resins in the use of FRP (Fibre Reinforced Polymer) especially for application to masonry, the new system known as FRCM (Fabric Reinforced Cementitious Matrix) was developed. This strengthening technique is usually composed of open fabric meshes embedded in inorganic matrices, as cemented-based mortar.

Both externally bonded reinforcement (EBR) FRP and FRCM systems allow to attain successfully the flexural and shear strengthening of concrete members and masonry walls, however, the premature debonding of composite sheets from the substrate surface can limit their effectiveness [1–5]. In particular, this type of failure may occur due to the low tensile strength of the substrate (concrete or masonry) that can therefore crack or to the weak bond strength at the interface between the composite system and the substrate. In general, the debonding failure does not allow to use the entire resistance of the strengthening system, furthermore it is a brittle failure that must be avoided especially when ductility is required for the structural behaviour, as in seismic upgrading. To prevent or delay the debonding of the EBR, it is necessary to insert anchoring systems, that can be realized by FRP strips, steel plates, bolts, composite connectors [6–15].

Among all the anchoring systems, the connectors made of dry fibres, also referred to as anchors, dowels or anchor spikes, are very versatile as they can be applied to different elements (beams, slabs, columns, walls) and materials (RC, masonry, wood), with different techniques (FRP and FRCM). The role of the anchor spikes for improving the performance of the strengthening system has been widely studied by different research groups based on experimental campaigns performed in the literature both on RC and masonry elements.

Nowadays, the application of FRP connectors is covered in the CNR-DT 200/2013 [16] and in the Fib Bulletin 90 [17]; but also for FRCM the

---

use of connectors is prescribed as provided in CNR-DT 215/2018 Italian guidelines [18] and in international standards ACI 549 Design Guidelines [19].

Even if the experimental evidence and the code provisions indicate that an improvement of the performance can be realized by the introduction of the anchoring devices, indications for the qualification of the material are still under study.

In this perspective, the article presents the results of a large experimental campaign carried out at the University of Sannio in agreement with the CNR-ITC (Construction Technologies Institute of the Italian National Research Council) to determine the mechanical characteristics of rovings for connectors made with bundles of dry fibres of different materials, under normal (ambient) conditions and after environmental conditioning to verify the durability and effects of ageing. The durability of fibres, investigated in this paper through tests in various environmental conditioning, is important to understand the performances of the different materials and thus to better choose the type (mortar or resin) and amount of coating for their use as connectors in different applications (masonry, concrete) and exposure of the structure. Using the results of these tests, the European Technical Assessment (ETA) [20] was issued in compliance with the European Assessment Document (EAD) [21]. Therefore, the application of this type of mechanical anchorages and the ETA evaluations are briefly summarized in the following before discussing the experimental results.

2. Assessment of steel and fibre rovings used for anchor spikes

Anchor spikes are strands of unidirectional bundles of carbon, glass, aramid, steel fibres held by a special net which gives to the connector (dowel) a cylindrical shape before its impregnation. The extremity, instead, is left free (fan) to be impregnated in situ and fanned over the fabric or the reinforcing mesh that has to be anchored. In particular, in case of FRP and FCRM application on RC and masonry, the dowel is inserted in a hole in the substrate and the fibres of the fan are splayed over the reinforcing system and then impregnated by epoxy or mortar (Fig. 1a). A similar anchorage configuration is mentioned in fib bulletin 14 [22] and more recently in fib bulletin 90 [17].

Since they can be perfectly integrated with the anchored FRP matrix, they can be manufactured to overcome various geometric complexities, moreover the possibility of manufacturing the connectors with the same materials of the external reinforcement facilitates the construction and eliminates the potential risks of corrosion from different materials.

Anchor spikes are commonly installed orthogonal to or in-plane with the reinforcement system, termed 90° and 180° (straight) anchor spikes respectively (Fig. 1a and b). It is worth noting that 180° anchor spikes are typically used to anchor FRP strengthening systems where geometric complexities in concrete members require that the FRP sheet or plate must be discontinued, whereas 90° anchor spikes are typically used for anchorage throughout the length of the FRP laminate, or near its termination [23].

However, different configurations can be adopted (Fig. 2) according to variable angles and radius of splaying of the fibres over the reinforcement, embedment lengths and angles of inclination of the dowel, number of fans, and type of fibres (glass, carbon, steel) [7,8,23–26].

The application of the connectors can be aimed at one end or intermediate anchorage generally in RC beams and columns to achieve greater efficiency in flexural, shear and confinement strengthening. But in case of masonry walls, they can be used to anchor FRP strips or to connect the layers of FRCM; one or two layers of FRCM can be connected to the wall for the entire surface to ensure the collaboration between the existing structure and the strengthening system (Fig. 3). A state-of-the-art review on the anchorage devices used to improve the efficiency of FRP EBR systems is provided in Refs. [15,23].

In case of FRCM systems applied to masonry panels or arches, the dowels are embedded or pass the entire thickness of the wall and the fans are splayed on one side or on both sides, respectively.

Therefore, they prevent slip and debonding of the new thickness from the masonry substrate increasing the wall lateral confinement and, accordingly, its compressive strength [27]. As a result, the reinforcement system has a confinement effect on masonry walls for the vertical loads and a double effect under seismic actions: increasing of the bending strength and ductility for out-of-plane actions and improving of the shear and flexural strength for in-plane actions. With reference to the in-plane shear behaviour of masonry reinforced with FRCM systems, the use of the anchors seemed to improve the post-peak behaviour of the masonry panels more than the capacity, leading to a more ductile behaviour without a relevant increase in shear strength [28].

Understanding the behaviour of connectors under different types of loads is a key aspect that should be considered during their design in order to predict the type of failure that can be attained.

Spike anchors can be subjected to pull-out forces or shear forces or combination of both, depending on the geometrical configuration and load pattern of the reinforced element. They may also be subjected to bending depending on the details of shear transfer through the attachment. Fig. 4 shows anchors spikes mainly subjected to shear (A) and pull-out forces (B), respectively.

The operating principle of anchor spikes is similar to that of adhesive anchors and depends on the transfer of tension loads from the embedment element to the substrate through a chemical bond and mechanical strength, therefore the behaviour of the connectors is generally affected by the embedment depth of the anchor [24,29].

As well as the ultimate load capacity, the embedment depth of the anchor dowel also influences the failure type. In summary an insufficient depth could cause concrete cone failure (CC) or mixed failure (CB) or adherent failure (BF) as shown in Fig. 5. Instead, a sufficient depth could produce bending failure (BD) or fibre rupture (FR).

However, the capacity of the anchor spikes depends not only on the embedment depth but also on the tensile strength of the substrate, the
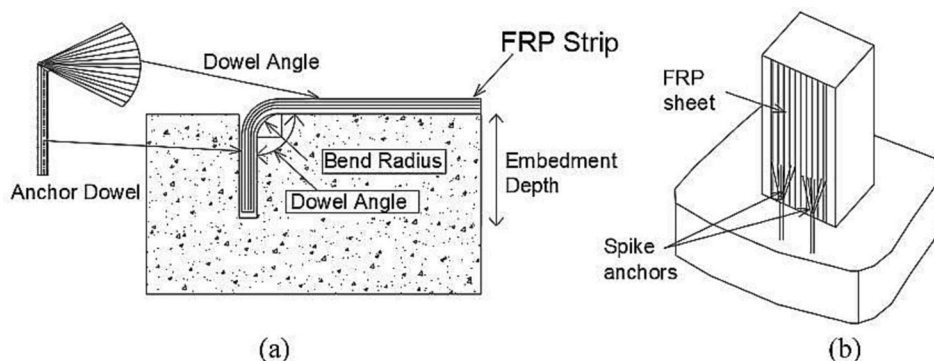

Fig. 1. Example of anchor spikes placed at 90° with the FRP (a) and 180° with the FRP (b).

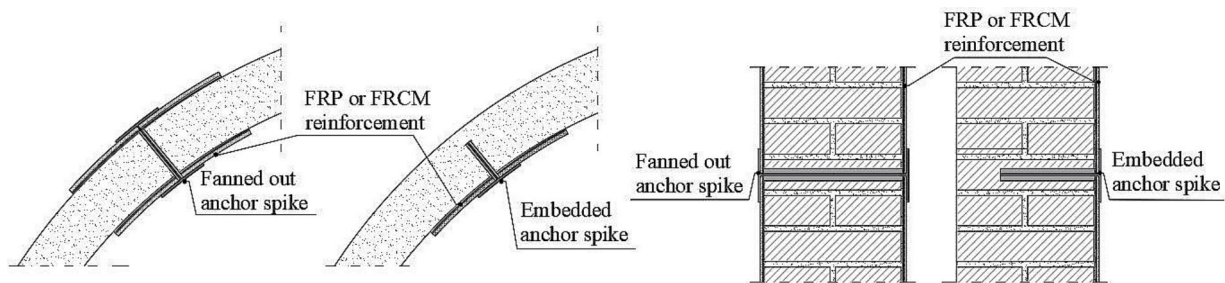Fig. 2. Different splaying configurations of the fan.

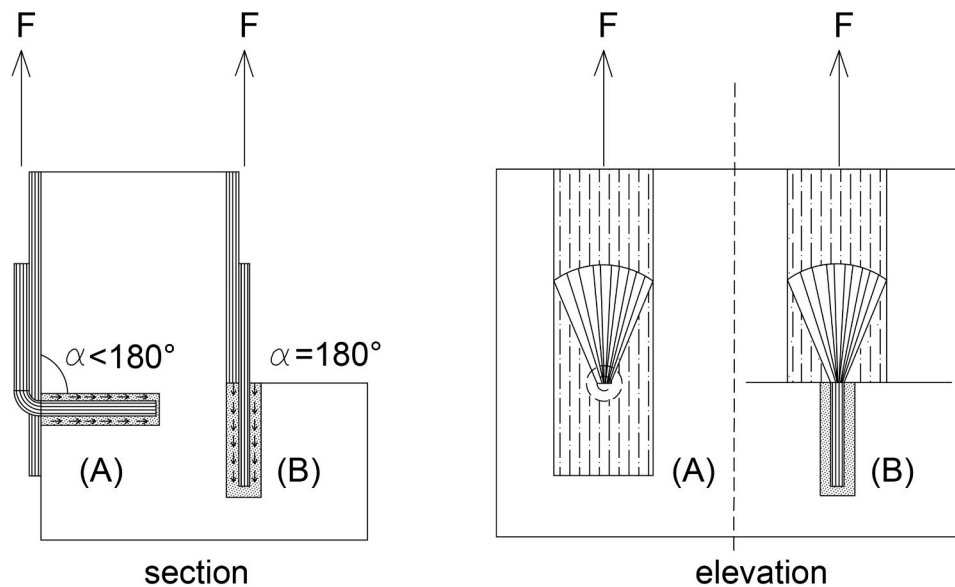Fig. 3. Example of application to arches (left) and masonry panels (right).

Fig. 4. Anchor spikes in different constructive configurations subjected to different type of load: (A) shear stress; (B) pull-out stress.

dimensions of the dowel and the hole in which it is connected [30], the strength of the material [31], furthermore its efficiency is influenced by details and accuracy of application procedures [32].

Experimental tests using various configurations have shown that the anchorages are effective in terms of deformability and strength increase, characteristics which are dependent on the number of anchorages used [25]. However, using many anchors with a short spacing can cause the failure of the reinforcement due to stress concentration around the hole [33].

Based on experimental results, several researchers [34–37] have developed analytical models to predict the performance of adhesive anchors in different applications, really related to the failure of the embedding material. Furthermore, some formulations for predicting the improvement of debonding load when the anchor is subjected to pull-out-force are provided in literature [38,39] according to the embedded depth of the connectors, although no design indications are currently available in case of shear loads.

At this point it is right to underline that the realization of the final application and its efficiency require experimental tests on the strengthening system that allow to evaluate the response of the anchors under the complex stress states presented in Fig. 4, i.e. pull out tests [18, 33,34], bending tests [40,41] or shear tests [6,15,26] that also simulate what could happen during an earthquake. However, the qualification of the material of the spikes is necessary anyway but specific procedures
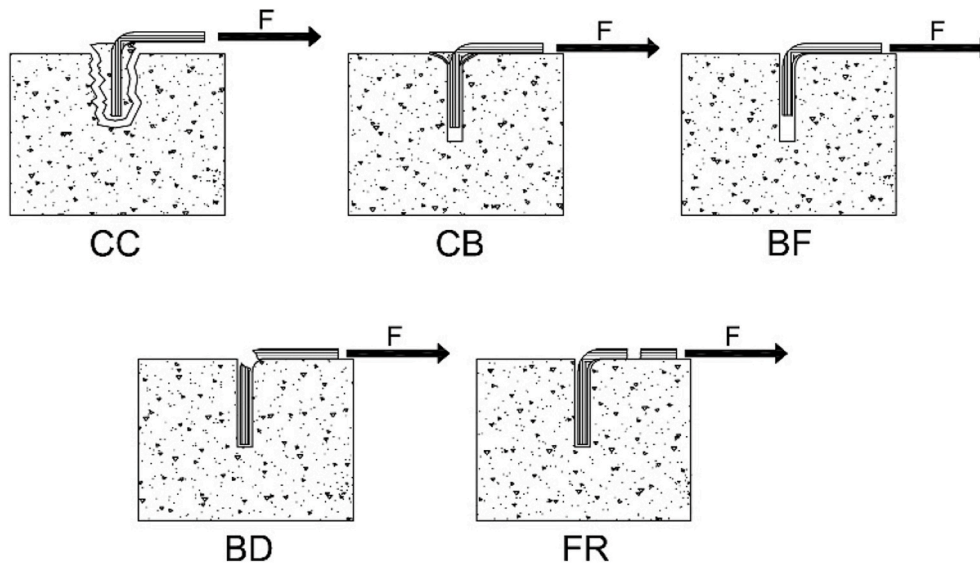
Fig. 5. Failure modes of anchor.

for the mechanical tests and limit of acceptability are not currently available. Therefore, the experimental tests presented in this paper were carried out for issuing the European Technical Assessment ETA 19/0361 of October 16, 2019 described in the following subsection.

2.1. ETA evaluations

ETA 19/0361 [20], issued by ITC-CNR, covers the assessment of the essential characteristics of a specific construction product in accordance with its respective EAD [21]; the latter includes all the methods of assessment of the characteristics and performance of the glass, basalt, aramid, carbon, PBO and steel rovings used for connectors.

Firstly, the technical description of the connectors and the mechanical characteristics to be measured are reported. The connector is described as "a bundle of continuous parallel strands/yarns" furthermore "the bundles of fibres/strands are collected within a tubular elastic net made of polyester, polyamide and latex yarns, that is extendable both longitudinally and transversely and removable. The bundle becomes rigid only after impregnation and hardening of the matrix (organic or inorganic)." The essential mechanical characteristics, identified in the EAD, are the tensile strength, the tensile modulus of elasticity and the ultimate strain. Furthermore, the performance evaluation under the following environmental conditions is assessable: alkali resistance in high pH solution, freezing and thawing, water resistance, saltwater resistance.

The constituting materials of the connectors are stated referring both to the properties of the fibres and steel strands and the properties of the bundles. In particular, the fibres are identified by means of the value of nominal Tex that counts the linear density of the yarn of the fibre, while the structure of the steel strands is defined by the number of wires.

The connector installation method, already described in the previous paragraph, is also reported specifying more in detail the steps to follow in order to allow a correct application of the system by the workers.

In the final part, the document shows the performance of the connectors defined through the results of the tests that have been carried out and described in this paper. It can be noticed that the mechanical properties are not the ones of the specific material but depend also on the geometry of the connectors and the experimental procedure, because the application of the tensile stress to a bundle of dry fibres does not allow a uniform distribution between all the fibres, therefore a great variability of the tensile strength can result depending on the size of the section (number of fibres).

3. Experimental program

3.1. Materials

The experimental program was aimed at determining the tensile strength, the elastic modulus and the ultimate strain of samples of dry fibre bundles that were collected within a tubular elastic net made of polyester, polyamide and latex yarns extendable both longitudinally and transversely and removable. The connectors were made of different materials (Fig. 6) and sizes:

– Galvanized steel (size 5, 8 and 10);
– Stainless steel (size 10);
– Aramid (size 6, 8, 10 e 12);
– Basalt (size 5, 8, 10 e 12);
– Carbon (size 6, 8, 10 e 12);
– AR-glass (size 6, 8, 10 e 12);
– E-glass (size 6, 8, 10 e 12);
– PBO (size 3 e 6).

Specifically, the size is a nominal value provided by the manufacturer which does not match the diameter of the dry anchor spike. Therefore, to define the mechanical properties of the dry connector the mean value of the cross sectional area [mm^2] is calculated from the weight of a piece of a bundle with the following relationship:

$$A_f = \frac{p_c}{\rho_c l_c} 1000 \tag{1}$$

where:

- l_c is the length of the piece of connector [mm].
- p_c is the weight of the dry material [g].
- ρ_c is the density of material [g/cm^3] provided by the manufacturer and reported in Table 1.

Accordingly, for the same size the connectors made of lower density materials are characterized by a higher fibre amount.

3.2. Specimens

The most difficult step of the experimental procedure concerned the preparation of the specimens that was widely investigated in various
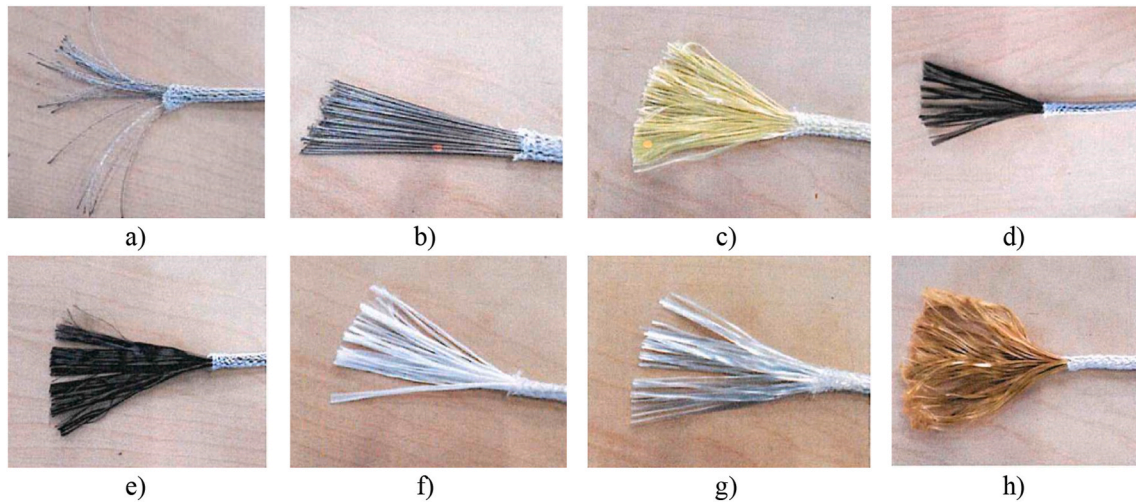
Fig. 6. Fibre bundles used in the experimental program: a) galvanized steel; b) stainless steel; c) aramid; d) basalt; e) carbon; f) AR-glass; g) E-glass; h) PBO.

Table 1
Density of materials used to manufacture anchor spikes.

Material	Steel	Aramid	Basalt	Carbon	AR-glass	E-glass	PBO
Density [g/cm^3]	7.85	1.44	2.67	1.81	2.68	2.66	1.56

experimental campaigns also in international Round Robin Tests [42]. To guarantee the alignment of the fibres and reduce the dispersion of the results due to the non-uniform distribution of the load to the fibres, a specific test procedure that involves the construction of steel sleeves at the ends of the connector (Fig. 7) was adopted. The sleeve, made with metal tubes of length $L_a = 30$ cm, allows to grasp the fibres in the grips of the tensile machine avoiding local breakages. The free length, L, of the connector to be tested is about 50 cm.

The preparation of the samples was carried out in two steps. During the first step, a piece of connector with a length of approximately 120 cm was placed on a wooden frame (Fig. 8) and lightly pulled to align the fibres, using steel rods. The upper and lower end of the connector, for a length of about 30 cm, were impregnated with two component resins over which, subsequently, a thin layer of quartz sand was applied to create a rough surface, and then they were embedded in two metal tubes with an external diameter of 21.3 mm filled with a two-component resin. After the technical times for the curing of the resins, the metal sleeve appears to be integral with the connector.

3.3. Environmental conditionings

Durability is an important property of construction materials that must have the capacity to keep their mechanical characteristics over time under the influence of external actions, since a deterioration of the structural components may affect the performance of the structure causing a premature failure. For these reasons it was essential to test the

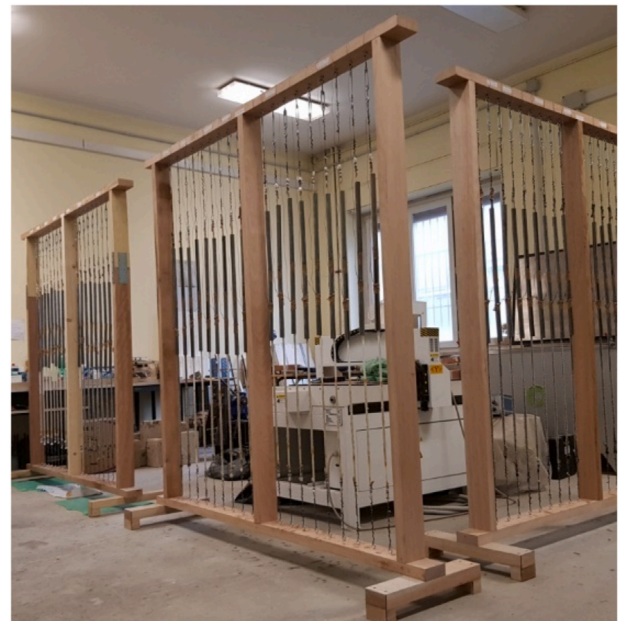**Fig. 8.** Wooden frames.

properties of the connectors after exposure to environments.

The exposure environments selected for this study, made in accordance with the reference standards, are the following ones:

a) Freezing and thawing

The environmental conditioning was carried out by submitting the samples for one week in a humidity chamber (100% humidity, 38 ±
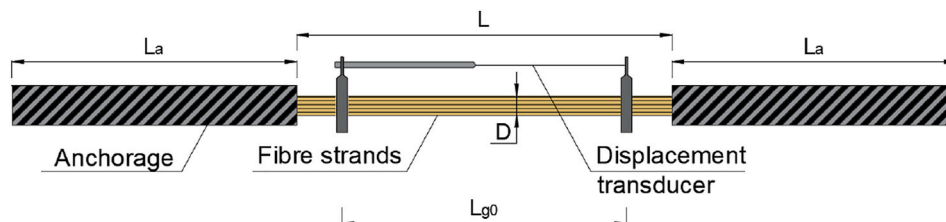

Fig. 7. Geometry of samples.

1 °C). Then, they were subjected to 20 freeze-thaw cycles. Each cycle consists of a minimum of 4 h at -18 ± 1 °C (Fig. 9a), followed by 12 h at 38 ± 1 °C and 100% controlled humidity (Fig. 9b).

b) Alkaline environment

Conditioning was done by immerging specimens in a liquid with pH = 13 (Fig. 10b) for 1000 and 3000 h at a temperature of 23 ± 2 °C (Fig. 10a).

c) Saltwater environment

The environmental conditioning was carried out by immerging specimens in saltwater according to ASTM D1141-98 [43] and ASTM C581-03 [44] for 1000 and 3000 h at a temperature of 23 ± 1 °C (Fig. 11).

d) Water environment

Conditioning was done according to ASTM D2247-11 [45] and ASTM E104-02 [46] immerging specimens in water for 1000 and 3000 h at a temperature of 38 ± 1 °C with a relative controlled humidity of 100% (Fig. 12).

After conditioning, the samples were tested in direct tension.

The summary of the tested specimens according to the type of environment is reported in Table 2. Five specimens were prepared for each size for the not conditioned tests, while the conditioned tests were performed on three specimens for the minimum and the maximum dimension of each material.

3.4. Methods and measurements

The specimens were subjected to direct tensile tests in displacement control (constant speed of 0.5 mm/min) with a universal machine (Fig. 13) and the sample was instrumented with a LVDT displacement transducer applied on the dry fibre with a measurement base of 350 mm (Fig. 7) in order to measure the strain and to evaluate the elastic modulus. The load was measured by a load cell with a maximum capacity of 600 kN.

For each specimen the tensile strength, the elastic modulus and the strain at maximum load were measured, both under normal conditions and after environmental conditioning. In particular, the tensile strength was calculated as the ratio between the maximum measured force and the cross-sectional area of the bundle equivalent in weight (A_f) as per equation (1). The tensile modulus E was calculated by the following expression:

$$E = \frac{\Delta F}{A_f} \frac{L}{\Delta L} 10^{-3} \tag{2}$$

where:

- ΔF and ΔL are the variation of the force [N] and of the length of the specimen [mm], respectively, between the two selected point of the load-displacement curve corresponding to the 10% and 70% of the maximum load;
- A_f is the cross-sectional area of the bundle [mm^2] calculated according to (1);
- L is the length of the specimen [mm].

The strain at maximum load ε_u is calculated from the following equation:

$$\varepsilon_u = \frac{L_{ga,f} - L_{ga,0}}{L_{ga,0}} \tag{3}$$

where:

- $L_{ga,f}$ is the length measured by the displacement transducer at maximum load [mm].
- $L_{ga,0}$ is the length measured by the displacement transducer at zero load [mm].

Fig. 14 shows the typical failure mode of the samples obtained after testing.

4. Results and discussion

4.1. NC specimens

The mean value of the tensile strength f_m [MPa], the mean modulus of elasticity E_m [GPa] and the mean value of the ultimate strain $\varepsilon_{m,u}$ [%] were determined for each material and size of the spikes without conditioning.

Table 3 shows the average values of the mechanical characteristics of not-conditioned (NC) specimens and the associated coefficient of variation (COV) reported in brackets for each cross-sectional area A_f.

From the results of the NC specimens the first observation regards the

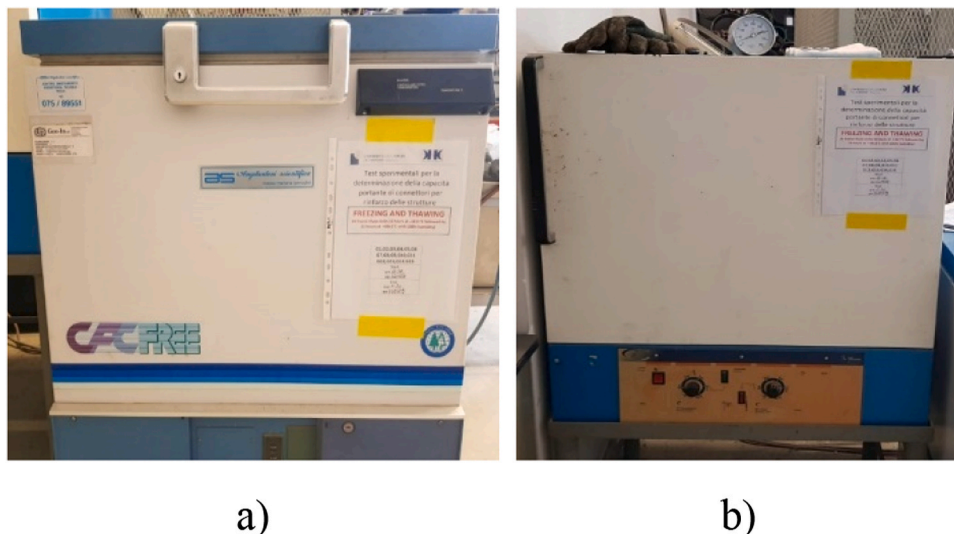a)   b)

Fig. 9. Equipment for freezing and thawing: a) freezer; b) temperature and humidity chamber.
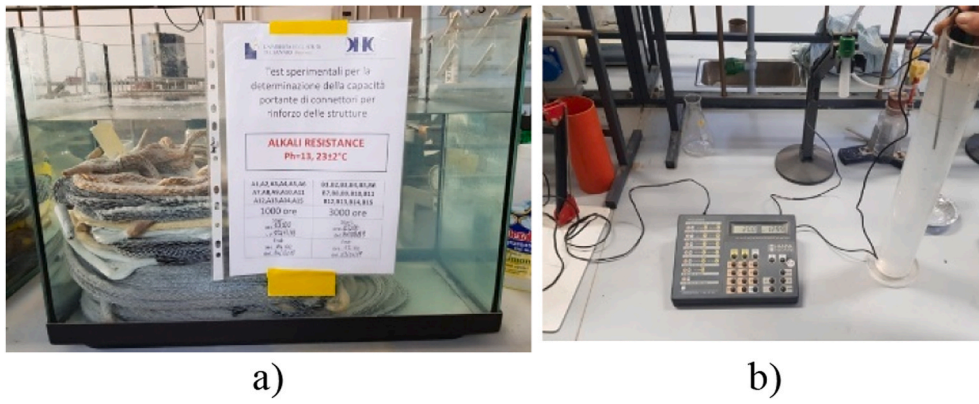
Fig. 10. Equipment for alkaline environment: a) glass case containing the connectors conditioned in alkaline environment; b) digital reader for checking the pH.

Fig. 11. Equipment for saltwater environment.

Table 2
Summary of tests.

Environmental conditioning	Abbreviation	Duration	Minimum number of specimens for each size
No conditioning	NC	None	5
	TOTAL		**5**
Freezing and thawing	F/T	20 cycles	3
	TOTAL		**3**
Alkaline environment	AR1000	1000 h	3
	AR3000	3000 h	3
	TOTAL		**6**
Saltwater environment	SR1000	1000 h	3
	SR3000	3000 h	3
	TOTAL		**6**
Water environment	WR1000	1000 h	3
	WR3000	3000 h	3
	TOTAL		**6**

Fig. 12. Equipment for water environment at controlled humidity.

relationship between the cross-sectional area, A_f, and the mean tensile strength, f_m, (Fig. 15). It is noted that for E-glass the tensile strength decreases when the area increases, while for galvanized steel the effect is less evident. Indeed, as the cross-sectional area of the composite connector increases, the resin used to integrate the metal sleeve to the anchor spike is not able to impregnate the connector core and increases the difficulty to perfectly align the fibres, preventing uniform inter-laminar transfer of the stresses and returning more dispersed results (high COVs for E-glass). The reduction of tensile strength with increasing diameter is a typical behaviour of FRP bars, as demonstrated by various tests available in the literature [47,48]. The tensile strength
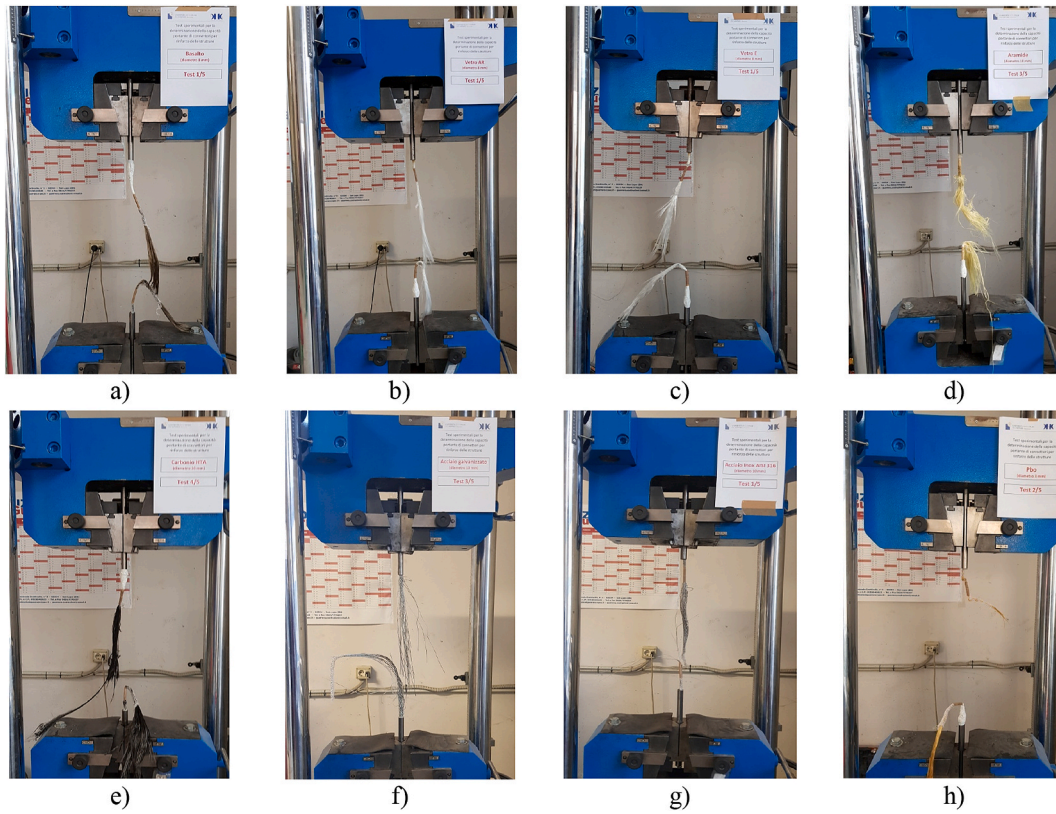

Fig. 13. Tensile-testing machine.

Fig. 14. Failure of anchor spikes: a) basalt size 8; b) AR-glass size 8; c) E-glass size 8; d) aramid size 10; e) carbon size 10; f) galvanized steel size 10; g) stainless steel size 10; h) PBO size 3.

Table 3
Mean values of mechanical characteristics of NC specimens.

| Material	Size	A_f [mm²]	f_m [MPa]		E_m [GPa]		$\varepsilon_{m,u}$ [%]	
Galvanized steel	5	9.68	2205	(6%)	230	(1%)	2.28	(5%)
	8	15.29	2141	(4%)	200	(4%)	2.28	(2%)
	10	18.73	2176	(4%)	207	(4%)	2.38	(6%)
Stainless steel	10	25.31	1369	(1%)	201	(3%)	2.34	(3%)
Aramid	6	20.83	1695	(10%)	112	(8%)	2.86	(9%)
	8	26.39	1699	(7%)	99	(5%)	2.86	(15%)
	10	33.33	1862	(6%)	163	(5%)	3.52	(4%)
	12	38.43	1826	(10%)	123	(8%)	3.50	(12%)
Basalt	5	12.98	667	(5%)	83	(9%)	0.97	(7%)
	8	19.73	677	(7%)	85	(4%)	1.14	(24%)
	10	25.22	850	(8%)	84	(4%)	1.56	(17%)
	12	31.46	708	(7%)	81	(14%)	1.35	(14%)
Carbon	6	15.84	1494	(5%)	234	(4%)	0.87	(9%)
	8	20.63	1573	(7%)	236	(3%)	0.82	(14%)
	10	28.73	1380	(5%)	232	(7%)	0.87	(18%)
	12	31.68	1429	(5%)	198	(2%)	0.94	(5%)
AR-glass	6	16.17	920	(9%)	86	(9%)	0.90	(13%)
	8	20.40	940	(6%)	85	(5%)	0.91	(9%)
	10	26.87	955	(8%)	77	(8%)	1.05	(7%)
	12	32.59	899	(7%)	84	(10%)	1.37	(14%)
E-glass	6	15.54	913	(4%)	93	(4%)	1.23	(9%)
	8	21.55	575	(11%)	66	(13%)	1.23	(15%)
	10	24.56	656	(11%)	68	(6%)	1.20	(11%)
	12	34.09	668	(11%)	64	(15%)	1.66	(17%)
PBO	3	11.54	2789	(6%)	198	(7%)	2.83	(10%)
	6	20.51	2983	(16%)	238	(7%)	3.09	(16%)
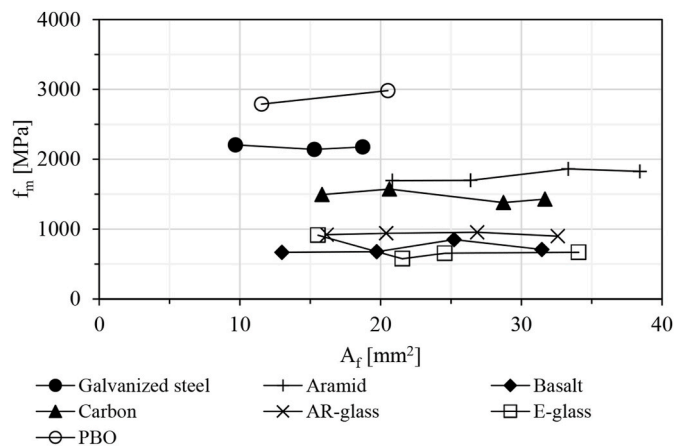
Fig. 15. Experimental data of tensile strength for each material according to A_f.

of FRP rebar depends on the diameter and the gripping system because the stress developed at the surface is not fully transferred to the fibres located in the core of the bar.

The same behaviour occurs for the connectors made of basalt, carbon and AR-glass but only for the greatest size for which the alignment of the fibres during the preparation of the specimens is more complicated. However, in general, the tensile strength is almost constant by varying the dimension of the connectors section, therefore the following analyses are carried out for the material type of the specimens considering the connectors with different dimensions all together. The same considerations can be made for the elastic modulus and the ultimate strain.

The statistical test of Shapiro-Wilk was performed to assess the normality of the experimental data. The analysis showed that the tensile strength values for each material come from a normally distributed population with a confidence level of 95%. Therefore, assuming a normal distribution and considering for each material the mean strength of all connectors it was possible to calculate the characteristic value of the tensile strength f_k [MPa]. The characteristic value was determined as indicated in EN 1990 [49] according to the following relation:

$$f_k = f_m(1 - k_n \cdot COV) \tag{4}$$

where COV is the coefficient of variation calculated as the well-known ratio between the standard deviation and the mean value, and k_n is a factor depending on the number of samples, reported in table D1 (V_x unknown) of EN 1990, Annex D.

The average value and the characteristic value of the tensile strength, the average value of the elastic modulus and the average value of the ultimate strain with the respective coefficients of variation for each material are reported in Table 4. Regarding the performance of the material, the PBO connectors show the greatest tensile strength and high stiffness and deformation capacity, while basalt ones show in general the worst mechanical response. It is worth noticing that the E-glass anchor spikes show the greatest scattering of the results (COVs up to 21%) while the stainless steel anchor spikes the lowest one (COV = 1%). In general,

the values of the ultimate strain are affected by greater dispersion compared to the other mechanical characteristics except for the anchor spikes made of galvanized steel, stainless steel, and aramid.

Regarding the characteristic value of tensile strength (Fig. 16), it is noted that the E-glass anchor spikes have the greatest penalization on the strength due to their highest scattering (37% reduction of f_k compared to the average value f_m). Furthermore, the value of f_k for the stainless steel and PBO anchor spikes is reduced about 25% compared to f_m due to the smaller number of tested specimens which determines higher values of the parameter k_n.

4.2. Effect of conditioning

In this section the results of the tensile test after the exposure of the anchor spikes to the different environments are discussed. To understand how the environments influence the tensile characteristics of the connectors, the results of the conditioned (C) samples exposed to freezing/thawing (FT), alkaline environment for 1000 h (AR1000) and for 3000 h (AR3000), saltwater environment for 1000 h (SR1000) and 3000 h (SR3000), water environment for 1000 h (WR1000) and 3000 h (WR3000) are compared with those of the NC samples.
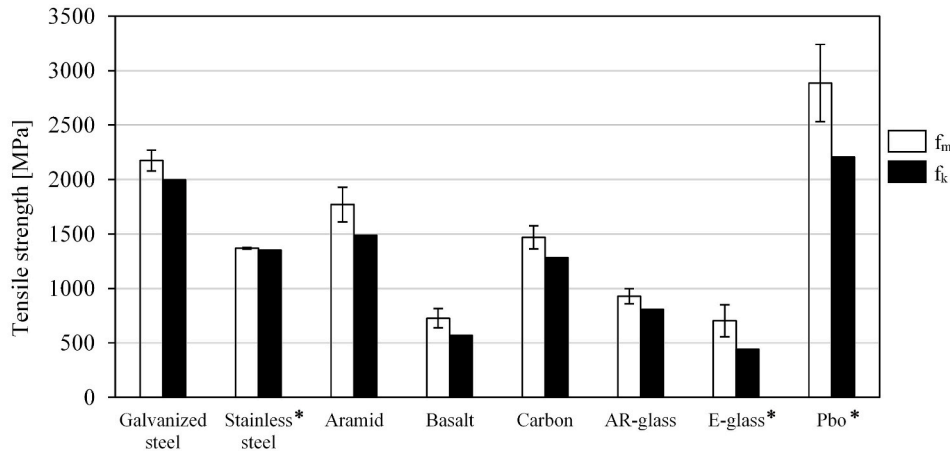
Tables 5 and 6 show, respectively, the trends of the ratio f_{mC}/f_{mNC} and E_{mC}/E_{mNC} for all the conditioning tests depending on the material of the anchor spikes. The coefficient of variation values referred both to tests on conditioned specimens (COV_C) and tests under normal conditions (COV_{NC}) are also reported.

From Table 5 it is noted that the freezing and thawing treatment less affects the tensile strength of the anchor spikes. Considering the other exposures, galvanized steel has a much greater reduction in resistance ($f_{mC}/f_{mNC} = 0.12$), although in some cases it shows COV up to 44%. Similar considerations were obtained for the E-glass connectors. Moreover, it is worth noticing that the environmental conditioning does not seem to reduce the strength of the stainless steel anchor spikes. Regarding the basalt fibres, the conditioning in alkali and salt water exposures affect less the tensile strength. This result is quite coherent with the chemical studies that established a good performance of basalt to alkali [50,51] and salt water [52].

The effect of conditioning on the stiffness of the connectors is reported in Table 6. In general, the tensile modulus shows lower scattering (COV = 0.5–41%) than the tensile strength. In many cases, such as for carbon, AR-glass and E-glass, the conditioning gives a limited reduction of the tensile modulus; the worst response of galvanized steel is confirmed.

The worst behaviour of galvanized steel is due both to the fabrication process and the preparation method of the specimens. Galvanizing is adopted to increase durability by reducing the risk of corrosion, however the coating is attached by environmental conditions especially salt water [53], furthermore the imperfections of the surface coating can allow the penetration of salt water to the steel. Therefore, the degradation of steel was due to the coating consumption but probably the bent of the specimen during the preparation contributed to local damage of the coating favouring the steel corrosion.

Regarding the dispersions of the results, the conditioned specimens

Table 4
Mechanical characteristics of NC specimens according to material.

Material	Galvanized steel	Stainless steel	Aramid	Basalt	Carbon	AR-glass	E-glass	PBO
f_m [MPa]	2174	1369	1770	726	1469	929	703	2886
COV [%]	4	1	9	12	7	7	21	12
f_k [MPa]	1998	1350	1491	570	1283	808	483	2207
E_m [GPa]	212	201	124	83	225	83	73	218
COV [%]	7	3	21	8	8	9	19	12
$\varepsilon_{m,u}$ [%]	2.31	2.34	3.19	1.26	0.87	1.06	1.33	2.96
COV [%]	5	3	14	24	12	21	20	14

*The reduction of f_k compared to f_m is due to the high scattering for the E-glass anchor spikes and both to the high scattering and the small copiousness of the sample for the PBO anchor spikes. For stainless steel the reduction is due to the smaller number of tested specimens that determines higher values of the parameter k_n.

Fig. 16. Values of f_m (empty background) with respective standard deviation and f_k (continuous background) for NC specimens.

Table 5
Effect of conditioning on tensile strength.

Conditioning	Value	Galvanized steel	Stainless steel	Aramid	Basalt	Carbon	AR-glass	E-glass	PBO
NC	COV_{NC}	4%	1%	9%	12%	7%	7%	21%	12%
FT	COV_C	24%	15%	8%	14%	25%	11%	53%	11%
	f_{mC}/f_{mNC}	0.80	0.93	0.88	0.83	0.60	0.41	0.55	0.78
AR1000	COV_C	12%	2%	12%	13%	23%	9%	14%	16%
	f_{mC}/f_{mNC}	0.49	0.96	0.82	0.92	0.58	0.63	0.62	0.66
AR3000	COV_C	19%	5%	8%	8%	19%	13%	20%	13%
	f_{mC}/f_{mNC}	0.36	0.95	1.05	0.86	0.72	0.51	0.69	0.86
SR1000	COV_C	21%	9%	10%	20%	22%	17%	7%	20%
	f_{mC}/f_{mNC}	0.12	1.04	0.72	0.97	0.87	0.64	1.01	0.82
SR3000	COV_C	43%	20%	6%	30%	54%	62%	18%	56%
	f_{mC}/f_{mNC}	0.26	0.92	0.91	0.84	0.66	0.43	0.85	0.50
WR1000	COV_C	44%	4%	16%	27%	7%	12%	15%	12%
	f_{mC}/f_{mNC}	0.38	0.88	0.95	0.65	0.64	0.48	0.59	0.93
WR3000	COV_C	38%	11%	6%	16%	22%	19%	13%	11%
	f_{mC}/f_{mNC}	0.37	1.05	0.90	0.64	0.78	0.43	0.46	0.87

show higher value of COV compared to the ones tested under normal condition. This aspect might be due both to the poor alignment of the fibres during the test and to the discontinuous effect of aging through the core of the connector.

5. Assessment of the material partial factor

In this section the assessment of the partial safety factor for anchor spikes is reported according to the different materials tested. According to the EN 1990 [49], the design value of a material or product property can be expressed as:

$$X_d = \eta \frac{X_k}{\gamma_m} \qquad (5)$$

where X_d is the design value, X_k is the characteristic value (herein the 5th percentile of the probability distribution), η is a conversion factor associated to environmental conditions, and γ_m is the material partial factor. By neglecting in a first stage the conversion factor due to the

environmental effect (i.e., assuming $\eta = 1$), the material partial factor can be calculated as:

$$\gamma_m = X_k / X_d \qquad (6)$$

Since the Normal distribution is a suitable distribution law for the tensile strength both in ordinary and exposure conditions (level of significance of 5%), the theoretical 5th percentile value, f_k, is calculated as follows:

$$f_k = f_m (1 - 1.645 \cdot COV) \qquad (7)$$

being f_m and COV respectively the mean value and the coefficient of variation of the distribution of the tensile strength. As reported in Table 7, it is specified that characteristic value determined with the probabilistic approach slightly overestimates the experimental value of the characteristic strength assessed by testing according to (4) (maximum 4.4% for PBO). Therefore, the use of the 5th percentile of the probability distribution as characteristic strength does not imply significant errors in the evaluation of the material partial safety factor,

Table 6
Effect of conditioning on tensile modulus.

Conditioning	Value	Galvanized steel	Stainless steel	Aramid	Basalt	Carbon	AR-glass	E-glass	PBO
NC	COV_{NC}	7%	3%	21%	8%	8%	9%	19%	12%
FT	COV_C	38%	13%	7%	17%	10%	9%	9%	15%
	E_{mC}/E_{mNC}	0.84	0.56	0.82	0.87	0.85	0.88	1.15	0.91
AR1000	COV_C	10%	5%	11%	6%	12%	7%	5%	3%
	E_{mC}/E_{mNC}	0.61	0.76	0.80	0.99	0.81	0.88	1.03	1.15
AR3000	COV_C	8%	20%	3%	3%	6%	5%	1%	4%
	E_{mC}/E_{mNC}	0.57	0.71	0.80	1.03	1.05	0.85	1.09	0.95
SR1000	COV_C	30%	16%	6%	6%	13%	6%	3%	22%
	E_{mC}/E_{mNC}	0.45	0.66	0.77	0.95	0.98	0.83	1.02	0.97
SR3000	COV_C	13%	0.5%	3%	5%	5%	9%	11%	41%
	E_{mC}/E_{mNC}	0.51	0.98	0.79	0.92	1.05	0.80	0.90	0.53
WR1000	COV_C	9%	13%	4%	10%	3%	9%	9%	10%
	E_{mC}/E_{mNC}	0.60	0.60	0.75	0.87	1.06	0.83	0.94	1.00
WR3000	COV_C	7%	5%	15%	1%	5%	5%	4%	4%
	E_{mC}/E_{mNC}	0.63	0.83	0.86	1.03	1.03	0.88	1.06	0.98

Table 7
Comparison of f_k assessed by testing according to (4) and f_k determined with the probabilistic approach according to (7).

Material	Galvanized steel	Stainless steel	Aramid	Basalt	Carbon	AR-glass	E-glass	PBO
f_k for (4) [MPa]	1998	1350	1491	570	1283	808	442	2207
f_k for (7) [MPa]	2016	1355	1509	580	1295	816	459	2304
Percentage difference	0.9%	0.4%	1.2%	1.8%	0.9%	1.0%	3.8%	4.4%

rather more conservative values of γ_m are determined.

The corresponding design value, f_d, can be expressed as follows:

$$f_d = f_m(1 - \alpha_R \cdot \beta \cdot COV) \quad (8)$$

where α_R is the FORM (First Order Reliability Method) sensitivity factor for the resistance and β is the target reliability index assumed respectively equal to 0.8 and 3.8 (Consequences Class CC2, Reliability Class RC2, 50 years reference period for ultimate limit states according to EN 1990 [49]).

The partial safety factors γ'_m were derived from the experimental data of each type of connectors material, but also a simplified approach considering only one safety factor γ_m for all materials is proposed. The latter factor was calculated in order to generalize the assessment of the material variability and the statistical uncertainties for two categories of materials that are steel and fibres, regardless the type of steel or fibres. Therefore, a new probabilistic variable, that is the experimental tensile strength divided by the respective mean value (f/f_m) for each material, was considered evaluating its mean value and standard deviation. The
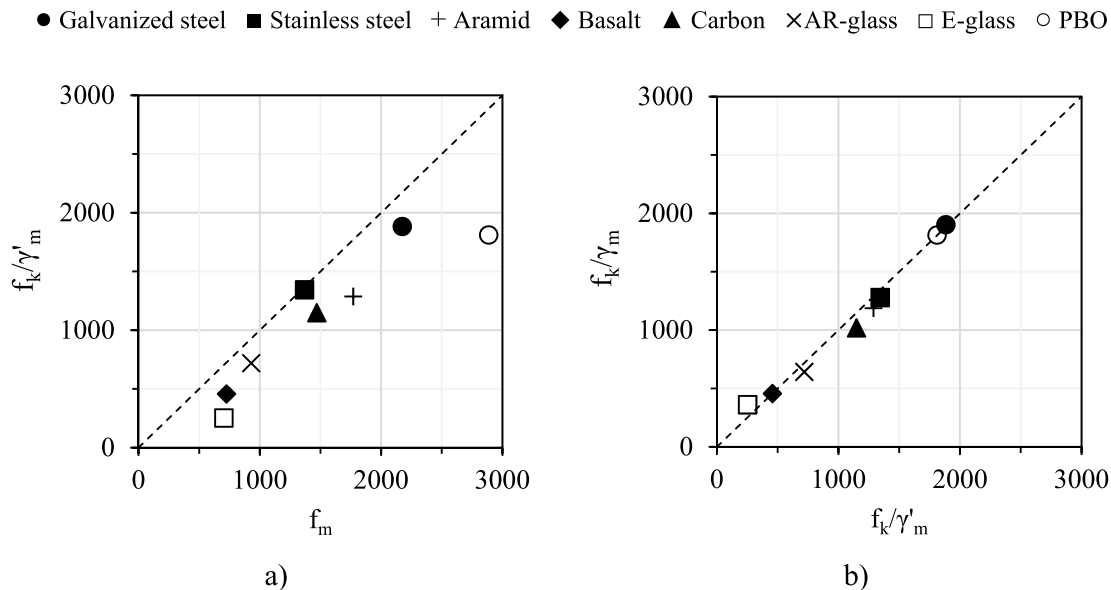

Fig. 17. Comparison between the design strength (f_k/γ'_m) and the mean strength f_m (a), and the design strength with partial safety factors evaluated for each material (γ'_m) or for categories of materials (γ_m) (b).

analysis of this new variable gave γ_m equal to 1.06 and 1.27 for the steel strands and the fibre based connectors, respectively. In Fig. 17a the comparison between f_k/γ'_m and f_m for each material is reported confirming that the design strength is safe for all the materials. Moreover, in Fig. 17b the comparison between f_k/γ_m and f_k/γ'_m is depicted for each material evidencing the goodness of considering only one partial safety factor both for all the steel connectors and the fibre ones.

In order to evaluate the environmental conversion factor, the ratio of the mean value of the tensile strength of C specimens over NC ones is calculated according to the empirical data of each material (Table 8). Specifically, in this case the freezing/thawing, alkaline, saltwater and water exposures were considered neglecting the effect of the different conditioning time because the results showed almost the same effect on degradation and stainless steel was excluded from the analysis because insensible to conditioning (Table 5). It is noted that the different types of conditioning variably influenced the value of the material properties, thus an average conversion factor η_{am} that considers the different exposures can be assumed for each material.

The results underline the best performance of basalt (0.80) and aramid (0.90) and the worst one of galvanized steel (0.45) and AR-glass (0.50).

6. Conclusion

The results of the experimental tests on anchor spikes made of various dry fibres give some information on the mechanical characteristics and durability of these systems. Firstly, it is important to underline that a standard test procedure was not available before these tests, therefore it was difficult to assess a reliable preparation of the specimens, but currently the ETA has been issued. It was necessary to apply a tensile force during the application of the end sleeves to realize a suitable alignment of the fibres avoiding a premature failure due to a non-uniform distribution of the stress in the "dry" section of the connector.

In this way the results obtained under normal conditions showed acceptable scattering in the range 1–20% giving significance results also in terms of dimension. In particular the main results are the following:

- the tensile strength and the elastic modulus are quite independent from the section dimension in all cases;
- PBO has the highest strength, but carbon has the greatest stiffness with a strength lower of approximately 50%;
- E-glass has the lowest stiffness.

Regarding the environmental conditioning to study the durability of the connectors, the results showed a high scattering in some cases; therefore, the test procedure has to be reviewed to guarantee the alignment of the fibres also after the treatment and the uniform effect of the aging through the core of the connector. However, some interesting results can be summarized:

- the freezing/thawing tests do not give relevant loss of resistance and stiffness for all the materials except for Carbon and E-glass; the stainless steel connectors are practically insensible to alkaline, saltwater and water environment.
- the galvanized steel connectors are much sensible to all the environment conditioning;
- E-glass is more sensible to alkaline and water treatment;
- basalt is less sensible to alkali and salt water;
- in all cases the results of degradation after 3000 h are quite the same of those after 1000 h.

The experimental results allowed to assess the partial safety factors $\gamma_m = 1.06$ and $\gamma_m = 1.27$ considering respectively all the type of steel strands and all the type of fibres based connector. Furthermore, the conditioned tests also allowed to evaluate the environmental factor η_{am} for each material that is variable in the range 0.45 (galvanized steel) -

Table 8
Environmental conversion factor.

Material	FT	AR	SR	WR	η_{am}
Galvanized steel	0.80	0.42	0.21	0.38	0.45
Aramid	0.88	0.93	0.81	0.92	0.90
Basalt	0.83	0.89	0.90	0.65	0.80
Carbon	0.60	0.65	0.77	0.71	0.70
AR-glass	0.41	0.57	0.54	0.46	0.50
E-glass	0.55	0.66	0.93	0.52	0.65
PBO	0.78	0.76	0.66	0.90	0.75

0.90 (aramid) excluding stainless steel that is practically insensible to conditioning.

These first results clearly indicate the different behaviour of the various materials that gives a provision for the design choice; however, it is necessary to understand the performance required to the connectors for each type of application to really choose the best solution.

CRediT authorship contribution statement

Giuseppe Maddaloni: Conceptualization, Methodology, Investigation, All authors have read and agreed to the published version of the manuscript. **Eliana Parcesepe:** Formal analysis, Data curation, Writing – original draft, preparation, All authors have read and agreed to the published version of the manuscript. **Annalisa Franco:** Methodology, Writing – original draft, preparation, All authors have read and agreed to the published version of the manuscript. **Antonio Bonati:** Methodology, Funding acquisition, All authors have read and agreed to the published version of the manuscript. **Antonio Occhiuzzi:** Supervision, Funding acquisition, All authors have read and agreed to the published version of the manuscript. **Maria Rosaria Pecce:** Conceptualization, Supervision, All authors have read and agreed to the published version of the manuscript.

Declaration of competing interest

The authors declare that they have no known competing financial interests or personal relationships that could have appeared to influence the work reported in this paper.

References

[1] Bonacci JF, Maalej F. Behavioral trends of RC beams strengthened with externally bonded FRP. J Compos Construct 2001;5(2):102–13.
[2] Triantafillou TC. Shear strengthening of reinforced concrete beams using epoxy-bonded FRP composites. ACI Struct J 1998;98(2):107–15.
[3] Cao SY, Chen JF, Teng JG, Hao Z, Chen J. Debonding in RC beams shear strengthened with complete FRP wraps. J Compos Construct 2005;9(5):417–28.
[4] Bilotta A, Ceroni F, Nigro E, Pecce M. Experimental tests on FRCM strengthening systems for tuff masonry elements. Construct Build Mater 2017;138:114–33.
[5] D'Antino T, Focacci F, Sneed LH, Christian Carloni. Relationship between the effective strain of PBO FRCM-strengthened RC beams and the debonding strain of direct shear tests. Eng Struct 2020;216:110631.
[6] Ceroni F, Pecce M, Matthys S, Taerwe L. Debonding strength and anchorage devices for reinforced concrete elements strengthened with FRP sheets. Compos B Eng 2008;39(3):429–41.
[7] Bournas DA, Pavese A, Tizani W. Tensile capacity of FRP anchors in connecting FRP and TRM sheets to concrete. Eng Struct 2015;82(1):72–81.
[8] Ceroni F. Bond tests to evaluate the effectiveness of anchoring devices for CFRP sheets epoxy bonded over masonry elements. Comp Part B 2017;113:317–30.
[9] Smith S, Zhang H, Wang Z. Influence of FRP anchors on the strength and ductility of FRP-strengthened RC slabs. Construct Build Mater 2013;49:998–1012.

[10] Niemitz CW, James R, Breña SF. Experimental behavior of carbon fiber-reinforced polymer CFRP sheets attached to concrete surfaces using CFRP anchors. J Compos Construct 2010;14(2):185–94.

[11] Zhang H, Smith S. FRP-to-concrete joint assemblages anchored with multiple FRP anchors. Compos Struct 2012;94(2):403–14.

[12] Mofidi A, Chaallal O, Benmokrane B, Kenneth N. Performance of end-anchorage systems for RC beams strengthened in shear with epoxy-bonded FRP. J Compos Constr ASCE 2012;16(3):322–31.

[13] Caggegi C, Pensée V, Fagone M, Cuomo M, Chevalier L. Experimental global analysis of the efficiency of carbon fiber anchors applied over CFRP strengthened bricks. Construct Build Mater 2014;53:203–12.

[14] Fagone M, Ranocchiai G, Caggegi C, Briccoli Bati S, Cuomo M. The efficiency of mechanical anchors in CFRP strengthening of masonry: an experimental analysis. Compos Part B 2014;64:1–15.

[15] Kalfat R, Al-Mahaidi R, Smith S. Anchorage devices used to improve the performance of reinforced concrete beams retrofitted with FRP composites: state-of-the-art review. J Compos Construct 2013;17(1):14–33.

[16] CNR DT 200/R1. Guide for the design and construction of externally bonded FRP systems for strengthening existing structures. Rome, Italy: Advisory Committee on Technical Recommendation for Construction of National Research council; 2013.

[17] Fib Bulletin 90. Externally applied FRP reinforcement for concrete structures, fib Task Group 5.1. Lausanne, Switzerland: International federation for structural concrete; 2019.

[18] CNR-DT 215/2018. Guide for the design and construction of externally bonded fibre reinforced inorganic matrix systems for strenghtening existing structures. Rome, Italy: Advisory Committee on Technical Recommendation for Construction of National Research council; 2018.

[19] ACI 549.4R-13. Guide to design and construction of externally bonded fabric-reinforced cementitious matrix (FRCM) system for repair and strengthening concrete and masonry structures. Farmington Hills, MI, USA: ACI committee 549, American Concrete Institute; 2013.

[20] ETA-19/0361 of 16/10/2019. Dalla Betta Group s.r.l., Glass, basalt, aramid, carbon, PBO and steel rovings for fibre-reinforced anchor spikes, issued by ITC-CNR, San Giuliano Milanese (Italy).

[21] EAD 331668-00-0601:06-2019, Glass, basalt, aramid, carbon, PBO and steel rovings for fibre-reinforced anchor spikes, EOTA, Pending for publication in OJEU.

[22] Fib Bullettin 14. FRP as externally bonded reinforcement of RC structures: basis of design and safety concept, fib Task Group 9.3. Lausanne, Switzerland: International federation for structural concrete; 2001.

[23] Grelle SV, Sneed LH. Review of anchorage systems for externally bonded FRP Laminates. Int J Concr Struct M 2013;7(1):17–33.

[24] Ozbakkaloglu T, Saatcioglu M. Tensile behavior of FRP anchors in concrete. J Compos Constr, ASCE 2009;13(2):82–92.

[25] Sun W, Liu H, Wang Y, He T. Impacts of configurations on the strength of FRP anchors. Compos Struct 2018;194:126–35.

[26] Llaurado PV, Fernandez Gomez J, Gonzalez Ramos FJ. Influence of geometrical and installation parameters on the behaviour of carbon fibre ropes embedded in concrete. Compos Struct 2017;176:105–16.

[27] Gago A, Proen J, Cardoso J, Cóias V, Paula R. Seismic strengthening of stone masonry walls with glass fiber reinforced polymer strips and mechanical anchorages. Exp Tech 2011;35(1):46–53.

[28] Ferretti F, Incerti A, Ferracuti B, Mazzotti C. FRCM strengthened masonry panels: the role of mechanical anchorages and symmetric layouts. Key Eng Mater 2017; 747:334–41.

[29] Akyuz U, Ozdemir G. Mechanical properties of CFRP anchorages. In: 13th world conference on earthquake engineering, Vancouver, B.C., Canada; 2004. Paper No. 3349.

[30] Maziligüney L, Yaman İÖ. Tensile behavior of chemically bonded post-installed anchors in low-strength reinforced concretes. In: 10th international congress on advances in civil engineering. Ankara, Turkey: Middle East Technical University; October 2012. p. 17–9.

[31] Lunn D, Rizkalla S. Design of FRP-strengthened infill-masonry walls subjected to out-of-plane loading. J Compos Construct 2014;18(3).

[32] Ceroni F, Pecce M. Evaluation of bond strength in concrete elements strengthened with CFRP sheets and anchorage devices. J Compos Construct 2010;14(5):521–30.

[33] Mutalib A, Hao H. Numerical analysis of FRP-composite-strengthened RC panels with anchorages against blast loads. J Perform Constr Facil 2011;25:360–72.

[34] Llaurado PV, Ibell T, Fernandez Gomez J, Gonzalez Ramos FJ. Pull-out and shear-strength models for FRP spike anchors. Compos B Eng 2017;116:239–52.

[35] Cook RA. Behavior of chemically bonded anchors. J Struct Eng 1993;119:2744–62.

[36] Marcon M, Vorel J, Ninčević K, Wan-Wendner R. Modeling adhesive anchors in a discrete element framework. Materials 2017;10.

[37] Eligehausen R, Cook RA. Appl J. Behavior and design of adhesive bonded anchors. ACI Struct J 2006;103(6):822–31.

[38] Orton SL, Jirsa JO, Bayrak O. Design considerations of carbon fiber anchors. ASCE J Compos Constr 2008;12(6):608–16.

[39] Özdemir G. Mechanical properties of CFRP anchorages. Master of Science Thesis. Istanbul Turkey: Middle East Technical University; 2005.

[40] Orton SL. Development of a CFRP system to provide continuity in existing reinforced concrete buildings vulnerable to progressive collapse. PhD Dissertation. Austin, TX: University of Texas at Austin; 2007.

[41] Sami Q, Ferrier E, Michel L, Si-Larbi A, Hamelin P. Experimental investigation of CF anchorage system used for seismic retrofitting of RC columns. In: Proceedings of the 5th international conference on FRP composites in civil engineering. Beijing: CICE; 27-29 Sept 2010.

[42] Bilotta A, Ceroni F, Barros JAO, Costa I, Palmieri A, Szabo ZK, et al. Bond of NSM FRP-strengthened concrete: Round Robin Test initiative. J Compos Construct 2016; 20(1). https://doi.org/10.1061/(ASCE)CC.1943-5614.0000579. http://hdl.handle.net/1854/LU-2940145.

[43] ASTM D1141-98. Standard practice for the preparation of substitute ocean water. West Conshohocken, PA: ASTM International; 2013.

[44] ASTM C581-03. Standard practice for determining chemical resistance of thermosetting resins used in glass-fiber-reinforced structures intended for liquid service. West Conshohocken, PA: ASTM International; 2003.

[45] ASTM D2247-11. Standard practice for testing water resistance of coatings in 100% relative humidity. West Conshohocken, PA: ASTM International; 2011.

[46] ASTM E104-02. Standard practice for maintaining constant relative humidity by means of aqueous solutions. West Conshohocken, PA: ASTM International; 2002.

[47] Cusson R, Xi Y. The behavior of fiber-reinforced polymer reinforcement in low temperature environmental climates. In: Tech. Rep. CDOT-DTD-R-2003-4. Department of Civil, Environmental & Architectural Engineering, University of Colorado; 2003.

[48] Achillides Z, Pilakoutas K. Bond behavior of fiber reinforced polymer bars under direct pullout conditions. J Compos Construct 2004;8(2):173–81.

[49] EN 1990:2002. Eurocode: basis of structural design. CEN; 2002.

[50] Ramachandran BE, Velpari V, Balasubramanian N. Chemicaldurability studies on basalt fibres. J Mater Sci 1981;16:3393–7.

[51] Tang C, Jiang H, Zhang X, Li G, Cui J. Corrosion behavior and mechanism of basalt fibers in sodium hydroxide solution. Materials 2018;11(8):1381.

[52] Zhang Q, Yan T, Luo L, Wang Q, Liu J. Effect of the properties of basalt fibers aging in salt solution. Conf Ser: Mater Sci Eng 2020;735:012049.

[53] Liu S, Zhao X, Zhao H, Sun H, Chen J. Corrosion performance of zinc coated steel in seawater environment. Chin J Oceanol Limnol 2016;35(2):423–30.